CERN/SPSC/77-12/
SPSC/P19/Add. 4/
17 February 1977

AN ADDENDUM TO THE NA4 PROPOSAL: SEARCH FOR MULTIMUON EVENTS

CERN-Dubna-Munich-Saclay Collaboration

ABSTRACT

A search for events in which several muons are simultaneously produced is justified on the basis of the recent experimental results on new particles and of the consequent theoretical developments. The length of our detector combined with the high intensity muon beam offers unique possibilities of searches for small cross-section phenomena. Narrow vector states of masses up to 20 GeV can be observed by their $\mu^+\mu^-$ decays with the carbon target option. A forward telescope provides tagging of the virtual photons.

1. PHYSICS MOTIVATIONS

1.1 Introduction

The so-called high-y anomaly observed in neutrino experiments[1] suggests the possible existence of new quarks (b-quarks) carrying a new flavour and being considerably heavier than the charmed quarks[2]. New quarks appear also as inevitable in many theories that seek unification of all interactions[3], the origin of CP-violation, the $\Delta I = \frac{1}{2}$ rule, and so forth. A fit to the neutrino data (Fig. 1) suggests that the mass of the new quark m_b, might be in the vicinity of 5 GeV. In complete analogy to the ψ, ψ' states, a new quark would most likely imply the existence of several narrow $(b\bar{b})$ states, which we shall denote by β, β', β'', and so on. For $m_b \geq 3.5$ GeV there might be as many as three such $3S_1$ states[4] below the threshold for the Zweig-allowed decays of $(b\bar{b})$, i.e. below pairs of $Y^+ \equiv (u\bar{b})$ and $Y^0 \equiv (d\bar{b})$ states (Fig. 2). The assumption that heavy quarks give rise to stronger binding is suggested by the observation that $\phi \equiv (s\bar{s})$ just fails to have a bound state, while $\psi \equiv (c\bar{c})$ has two of them. We expect the trend to become even more apparent at higher quark masses. One can calculate[4] within the charmonium model[5] the masses and widths of the β-states with a reasonable amount of confidence. Some of the masses and widths are summarized in Table 1. Decay schemes are shown in Fig. 3. Particularly relevant to our application, the decay branching ratio of the β-states into $\mu^+\mu^-$ is estimated to be $B_{\mu\mu} \simeq 4\%$.

Production of β-particles by muons proceeds through the exchange of an almost real photon, as shown in Fig. 4. Observation of the leading muon will be used to tag the energy of these photons. The cross-section for muon production is reduced with respect to photoproduction by a factor of the order of α, owing to the presence of the extra vertex. The effective photon flux has been expressed by Tsai[6] in terms of effective radiator thickness $X_{eq}(\nu, E_\nu)$, the slow varying function of the muon incident energy E_μ and of the photon energy $\nu = E_\mu - E_{\mu'}$. The number of photons per unit of energy is then given by the formula

$$\frac{dN}{d\nu} = X_{eq}(\nu, E_\mu)\,\frac{1}{\nu}\ .$$

The dependence of X_{eq} is shown in Fig. 5. We remark at this point that the smallness of X_{eq} is more than compensated by the fact that muons can traverse very thick targets without appreciable radiative losses.

The experimental results[7] of photoproduction of $\psi(3100)$ particles are shown in Fig. 6. The salient features are as follows:

i) The total cross-section is $\sigma[\gamma N \to \psi(3100) + X] \simeq 30$ nb;

ii) The t-dependence is of the type $e^{-4|t|}$;

iii) The process appears to be mainly diffractive.

In order to predict the cross-section for more massive objects we have extrapolated the cross-sections as $M^{-\alpha}$, where α is a parameter $\simeq 4\text{-}5$ [8,9]. The same $|t|$-dependence $e^{-4|t|}$ has been retained also for the heavier objects, limiting however the integral up to the kinematic limit t_{min}. The energy excitation curve has been scaled from $\psi(3100)$, shown in Fig. 6. Finally muon cross-sections have been obtained after integration over the virtual photon spectrum of Fig. 5. Results are listed in Table 2.

Since interesting values of (cross-section × branching ratio) are expected to be in the range 10^{-37}-10^{-40} cm^2 per nucleon, we must make use of the largest luminosity obtainable with our apparatus, i.e. it is advisable to run the experiment with the carbon target option[10]. Assuming 2×10^8 μ/pulse, 10^4 pulses/day, and a 50 m long high density carbon target, we get as a first order of magnitude estimate of the ultimate sensitivity of the detector the luminosity L = $= 2 \times 10^8 \times 10^4 \times 5 \times 10^3 \times 2.08 \times 6.06 \times 10^{23} = 1.3 \times 10^{40}$ cm^{-2} per day. Equivalently, one could hope to detect at the level of $\sim$ 1 event per day and 50% detection efficiency processes for which $\sigma \cdot B = 1.5 \times 10^{-40}$ cm^2. This sets at approximately 20 GeV the maximum value of the mass which can be observed with our apparatus (for $\alpha = 4$).

1.2 Target arrangement

The use of a carbon target has been discussed already in our original proposal[10]. Here we shall consider in more detail the effects of energy losses of beam particles through such a large amount of material, i.e. 10^4 g/cm^2. Besides ionization and excitation losses, muons lose energy because of:

i) Bremsstrahlung. The formula is[11]

$$-\left.\frac{dE}{dx}\right|_b = -4\,\alpha\,N\,r_e^2\,\frac{Z^2}{A}\left(\frac{m_e}{m}\right)^2 E\left[\ln\left(\frac{12EZ^{-\frac{1}{3}}}{5mc^2}\right) - \frac{1}{3}\right] .$$

where m is the muon mass. For E = 300 GeV, $\left.dE/dx\right|_b = 0.32$ MeV/g·cm^2.

ii) Electron pair production. The formula is[12]

$$-\left.\frac{dE}{dx}\right|_{e^+e^-} = -\frac{N}{A}\frac{m_e}{m}\frac{(\alpha Z r_e)^2}{\pi} E\left[19.3\,\ln\left(\frac{E}{mc^2}\right) - 53.7\right] f ,$$

where $f \leq 1$ is a term due to the screening effects. For E = 300 GeV

$$\left.\frac{dE}{dx}\right|_{e^+e^-} = 0.30 \text{ MeV/g}\cdot\text{cm}^2 .$$

iii) Nuclear interactions. The main process proceeds through almost real photons

$$-\left.\frac{dE}{dx}\right|_n = -\frac{2N}{\pi}\,\alpha\,\sigma_\gamma\,E ,$$

where σ_γ = 120 μb is the total photoproduction cross-section[13]. For $\sigma_{tot} \simeq 1$ μb, the probability of nuclear interaction of a muon traversing the whole target is 6×10^{-3}.

The total average energy loss of a 300 GeV muon traversing the whole target amounts to 30.7 GeV, of which about 12.3 GeV are due to losses other than ionization and excitation.

A second important effect is multiple Coulomb scattering. A pencil beam entering the target with E_μ = 250 GeV at the end of the spectrometer will have a r.m.s. radial displacement of 2.74 cm. Hence about 99% of this pencil beam will remain contained in a cylinder of 7 cm radius. However, the scattered particles have lost a greater fraction of this momentum and besides being emitted to finite angles are considerably affected by the multiple scattering. We propose to ensure containment within the target volume by surrounding the carbon with a relatively thin cylinder of magnetized iron acting like a reflecting mirror to particles incident on it at a relatively small angle. As one can see from Fig. 7, neglecting multiple scattering, the exit angle from the iron is equal to the one of incidence. Then the total path s inside the magnetized region must be the one required to build up twice the transverse momentum of the incident particle, i.e. $s = [p_T(\text{MeV/c})/300]$ m for B = 2 T. Since scattered particles are normally emitted at small angles (and relatively small p_T) they are literally bouncing off the iron pipe into the target again, until they reach the end of the apparatus. As pointed out in the original proposal[10], these oscillations, which are symmetric with respect to the main axis of the spectrometer, retain muons permanently trapped inside the magnetized iron, provided its thickness t is such that

$$t \geq \frac{M_p}{0.2\ B_0} \frac{q^2}{q^2_{max}} , \qquad \text{(units GeV, T, m)}$$

where q^2 is the value of the four-momentum transfer (the square of the mass) of the initial photon, $q^2_{max} = 2M_p E_\mu$ its maximum kinematically allowed, M_p is the proton mass, and B_0 is the (uniform) field inside the torus. For E_μ = 280 GeV, q^2_{max} = 525 GeV^2 and to ensure containment up to q^2 = 10 GeV^2, t = 3 cm. In practice, a slightly greater thickness is required to take into account the effects of multiple scattering and of the initial beam divergence (Fig. 8).

1.3 Tagging the energy of the virtual photons

The invariant mass of the virtual photon is limited by the requirement of containment inside the iron pipe. Its energy is determined with a simple detector to be added at the end of the apparatus, consisting of a bending magnet, a muon absorber, and an array of scintillation counters (Fig. 9). The total bending power is 8 T•m, corresponding to a transverse momentum kick of about 2.5 GeV/c.

The main unscattered beam will then be bent by about 10 mrad, corresponding to a 20 cm displacement 20 m downstream. Lower momentum particles, which presumably have been the result of a collision, are bent to a larger angle and if the virtual photon energy is sufficiently large are bent out of the main beam onto an array of tagging counters. A 2 m thick iron or concrete absorber is used to remove false triggers due to secondary pions coming through the pipe. The total rate of the tagging system is expected to be $\sim 10^{-3}$ times that of the incident beam, when photon energies $\nu = E_\mu - E'_\mu \geq 0.5\ E_\mu$ are selected.

1.4 Trigger, detection efficiency, and mass resolution

The trigger will require, in addition to the tagged photon of energy $\nu \geq \frac{1}{2} E_\mu$, the presence of at least a second muon of sign opposite to the one of the beam. The spectrometer polarity will be set such as to focus particles of the same sign as the incoming beam. Therefore the wrong sign muon will be deflected towards the periphery of the spectrometer and will inevitably hit the outer rings of some of the trigger counters. A typical event is shown in Fig. 10.

The reconstruction of the event will require that both focused and defocused tracks traverse at least 7 consecutive chamber planes, of which there are at least three in both the x- and y-directions. The detection efficiency has been estimated using a Monte Carlo simulation program, which takes into account the exact geometry of the apparatus. The result is shown in Fig. 11. It appears that β-objects of mass $M \geq 9$ GeV can be detected with an efficiency of not less than 50%.

The invariant mass resolution is mainly determined by the multiple Coulomb scattering in the iron of the magnet. The expected mass resolution is shown in Fig. 12. We remark that it is barely sufficient to separate out β, β' and β'' states, as long as they are ~ 400 MeV apart, as predicted from Fig. 2.

1.5 Backgrounds

Detecting a narrow peak at very large $\mu^+\mu^-$ masses is possible only as long as the continuum of muon pairs under the peak is not excessive. We have considered several possible sources of simple background events. The only effect one knows how to calculate reliably is the electromagnetic trident production, shown in Fig. 13. We have numerically integrated the relevant formula[14], taking into account the effects of nuclear form factors. The conclusion is that this background is rather small, as long as $B_{\mu\mu} \simeq 4\%$ and the cross-sections are those listed in Table 2. Another form of background can be due to the "direct" lepton production of the hadronic vertex (Fig. 14). A guess can be made of this background taking the experimental observation[15] at FNAL that $\sigma(p + p \to \mu^+\mu^- x) \simeq$ $\simeq 10^{-37}$ cm^2 for $E_p \simeq 400$ GeV and $M_{\mu\mu} \geq 10$ GeV. Since the total hadronic

cross-section of muons is $\sigma(\mu p \to \text{hadrons} + \mu) \simeq 10^{-30}$ cm^2, to be compared with $\sigma(pp \to \text{hadrons}) = 32$ mb, we can scale down the cross-section in one case by the amount $\sigma(\mu p \to \text{hadrons} + \mu)/\sigma(pp \to \text{hadrons}) \equiv 3 \times 10^{-5}$, giving an expected total cross-section for pairs of muons of the order of $10^{-37} \times 3 \times 10^{-5} \simeq 3 \times 10^{-42}$ for $M_{\mu\mu} > 10$ GeV, which is entirely negligible. We must stress, however, the very speculative nature of this argument and that in reality the background might indeed be more abundant.

Finally, we have considered the contributions of associated charm production. In the absence of more reliable data, we have made use of a simple quark-model[16]. At best, within this model, contributions appear negligible. We stress again the weak nature of such an argument.

In conclusion, the $\mu^+\mu^-$ continuum seems to be dominated by the e.m. trident production process, which is in any case smaller than the expected signal, at least under the invariant mass peak (Fig. 13).

1.6 Other observable physical processes

There may be several possible processes, which would lead to more than one muon in the final state that will be collected during the experiment. This offers sensitivity to several possible new phenomena. Amongst the interesting signatures there is the one in which three muons are emitted from the same point with no other visible track (quiet events) and as yet the sum of the energies of the three particles does not match the total beam energy. This missing energy can then be attributed to neutrinos. The process could be due to a heavy charged lepton pair

$$\mu^+ N \to L^+ + L^- + \mu^+ \text{ (leading track)} + N \text{ (spectator)}$$
$$\qquad\quad \downarrow \qquad\quad \hookrightarrow \mu^- \nu\nu$$
$$\qquad\quad \hookrightarrow \mu^+ \nu\nu$$

Cross-sections are estimated in the range 10^{-36}-10^{-37} cm^2 for $M_L \simeq 2$ GeV and decrease as M^{-4}. Therefore they fall within the general capability of our apparatus.

Another possibility, recently discussed[17], is the existence of a pair of neutral heavy leptons M_0, E_0 having only weak interactions and decaying into leptons

$$M_0, E_0 \to \mu^+\mu^-\nu \ .$$

The cross-section for production of such objects is estimated to be $\simeq 10^{-36}$ cm^2 at high energies.

It appears that in order to study these phenomena, the calorimetry around the target proposed in the original proposal[10] and later dismissed in the reduced

version of the apparatus should be revived again. We are actively considering this and we plan to submit the appropriate document to the Committee in the near future.

2. ADDITIONAL HARDWARE AND TIMETABLE

A relatively modest amount of new construction is required in order to extend our experimental programme along the lines of this new document:

i) Target. A carbon target was foreseen in the original proposal[10]. We now want to add an external magnetized iron cladding.

ii) Downstream tagging telescope. Three 2 m bending magnets are necessary. They are already at CERN and they can be made available. Power and cooling have to be provided. Tagging counters and electronics can be provided by the Collaboration.

These components can be ready at the same time as the main NA4 set-up and they will not interfere with the construction of the rest of the apparatus.

We would like to start our experiment with the carbon target. Because of the topical interest of our programme, we urge the Laboratory to schedule the search for multimuon events as soon as the beam becomes available.

APPENDIX I

List of participants in the NA4 experimental programme:

CERN : M. Bozzo, F. Ceradini, D. Cline*), F. Muller, B. Naroska, C. Rubbia**).

Dubna : I.A. Golutvin, I.M. Ivanchenko, Yu.T. Kiriouchine, V.S. Kiselev, V.G. Krivokhijine, V.V. Kukhtin, I. Manno, W.-D. Nowak, I.A. Savin, D.A. Smolin, G. Vesztergombi, A.G. Volodko, R.Ya. Zulkarneev.

Munich : J. Irion, F. Navach, U. Meyer-Berkhout, D. Schinzel***), H. Seebrunner, A. Staude, R. Tirler, R. Voss, Č. Zupančič.

Saclay : J. Feltesse, A. Lévêque, E. Pauli, J. Renardy, G. Smadja, M. Spiro, M. Detremmerie, J. Zsembery.

---

*) Visitor from University of Wisconsin, Madison, Wisc., USA.

**) Spokesman.

***) Alternative contact man.

REFERENCES

1) A. Benvenuti et al., Phys. Rev. Letters 34, 597 (1975).

2) R.M. Barnett, Phys. Rev. Letters 36, 1163 (1976), and SLAC-PUB-1821.

3) F. Gürsey and P. Sikivie, Phys. Rev. Letters 36, 775 (1976).

4) E. Eichten and K. Gottfried, Heavy quarks in e^+e^- annihilation, CNLS 350 (1976), and submitted to Physics Letters.

5) T. Appelquist and H.P. Politzer, Phys. Rev. Letters 34, 43 (1975).

6) Y.S. Tsai, Rev. Mod. Phys. 46, 815 (1974).

7) T. Nash et al., Phys. Rev. Letters 36, 1233 (1976), and other references therein.

8) S. Gerhstein and S. Geraskinov, private communication to I. Savin; they suggest $\alpha = 2$.

9) J. Ellis, private communication.

10) CERN/SPSC/74-79/P19, 1 August 1974.

11) E.P. George and A.C. Jason, Proc. Phys. Soc. A63, 1248 (1950).

12) E.P. George, Progr. Cosmic Ray Phys. 1, 395 (1952).

13) W.P. Hesse et al., Phys. Rev. Letters 25, 613 (1970).

14) S.J. Brodsky and S.C.C. Ting, program to compute trident cross-sections.

15) D.C. Hom et al., Phys. Rev. Letters 37, 1374 (1976).

16) V. Barger and R.J.N. Phillips, Dimuons from inelastic μN scattering, Wisconsin preprint COO-563 (1976).

17) V. Barger and D.V. Nanopoulos, $\mu \to e\gamma$: possible signature of heavy neutral leptons, Wisconsin preprint COO-583 (1977), submitted to Phys. Rev. Letters.
S.M. Bilenky and S.T. Petkov, On a possible suppression of parity violating effects in heavy atoms, Dubna preprint E2-10405 (1977).

Table 1

Decay widths of narrow states of type ($b\bar{b}$). From Ref. 4

		$\psi(3100)$	β	β'	β''	Units
Mass	M	3.1	10.0[a]	10.4	10.8	GeV
Total width	Γ_{had}	59	$\approx$ 16.0	?	?	keV
Leptonic width	Γ_{ee}	4.8	$\approx$ 0.7	0.5	0.4	keV
Branching ratio into $\mu^+\mu^-$	$B_{\mu^+\mu^-}$	0.07	0.04	$\lesssim$ 0.02	$<<$ 0.01	

a) Initial assumption.

Table 2

Cross-sections (cm^2) per nucleus for β muoproduction on p and on C

Reaction and power law[a] \ β mass (GeV)	3	6	9	12	15	18
$\mu p \to \mu\beta + X$						
M^{-5}	6.0×10^{-34}	6.8×10^{-36}	3×10^{-37}	1.9×10^{-38}	8×10^{-40}	6.5×10^{-42}
M^{-4}	6.0×10^{-34}	1.4×10^{-35}	9×10^{-37}	7.6×10^{-38}	4×10^{-39}	4×10^{-41}
$\mu C \to \mu\beta + X$						
M^{-5}	2×10^{-32}	2.2×10^{-34}	8.6×10^{-36}	4×10^{-37}	1.5×10^{-38}	1.1×10^{-40}
M^{-4}	2×10^{-32}	4.4×10^{-34}	2.5×10^{-35}	1.6×10^{-36}	7.5×10^{-38}	6.6×10^{-40}

a) $\sigma \propto M^{-\alpha}$ refers to the photoproduction process: γ target $\to \beta + X$.

Figure captions

Fig. 1 : Data from HPWF experiment on the high-y anomaly. Lines at $d' = 4$ and $d' = 5$ represent best fits to the data for $m_b = 4$ GeV and $m_b = 5$ GeV, respectively.

Fig. 2 : $b\bar{b}$ excitation energies as a function of quark mass.

Fig. 3 : $b\bar{b}$ decay spectrum for $m_b = 5$ GeV.
a) E_1 γ decays.
b) Hadronic decays.

Fig. 4 : Basic diagram of β production by muons.

Fig. 5 : Effective radiator thickness of muon beam.

Fig. 6 : Total cross-sections for ψ/J photoproduction.

Fig. 7 : Mirror action of a magnetized iron plate.

Fig. 8 : Schematics of target arrangement.

Fig. 9 : NA4 experimental apparatus with added tagging telescope.

Fig. 10 : Typical event: $E_{inc} = 300$ GeV, $M_{\mu\mu} = 12$ GeV; $E_\gamma = 150$ GeV.

Fig. 11 : Detection efficiency for $\mu + N \rightarrow \beta + X + \mu$, $\beta \rightarrow \mu^+\mu^-$

Fig. 12 : Expected mass resolution of NA4 apparatus for $\beta \rightarrow \mu^+\mu^-$.

Fig. 13 : Calculated trident and expected $\beta \rightarrow \mu^+\mu^-$ yields as a function of the dimuon invariant mass.

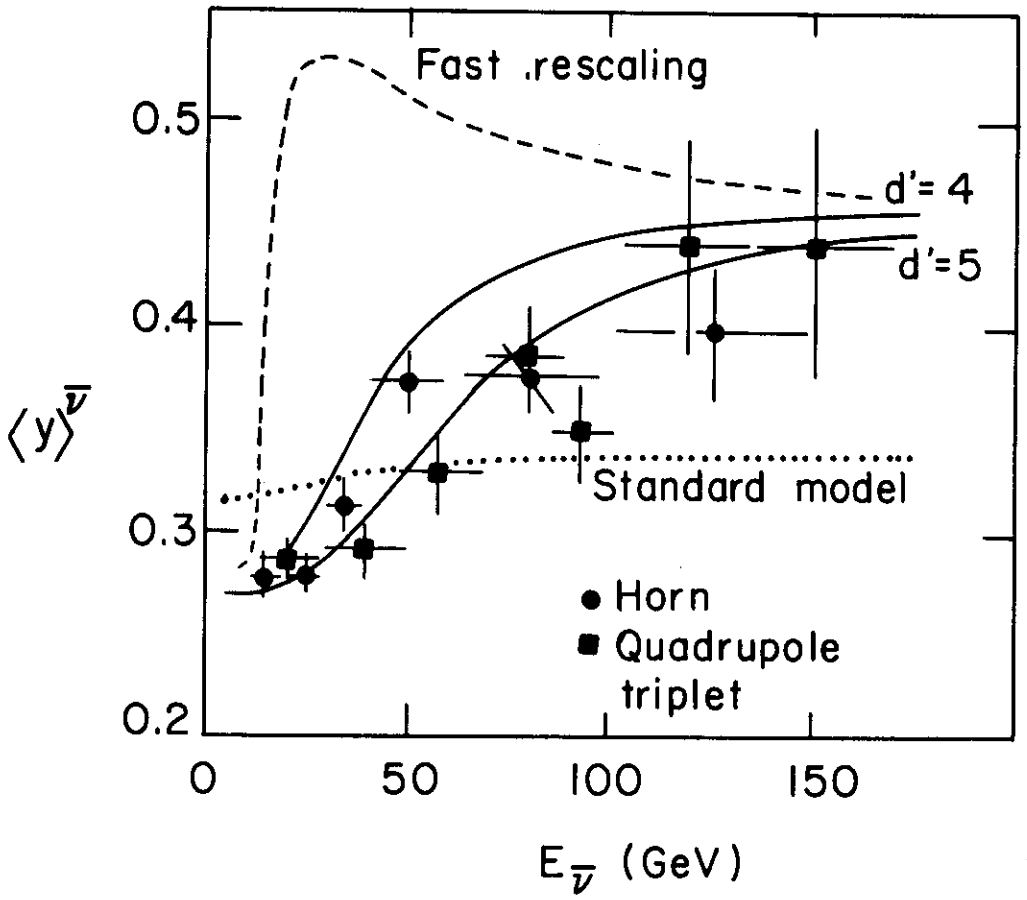
Fast rescaling
d'= 4
d'=5
Standard model
Horn
Quadrupole triplet
0.5
0.4
0.3
0.2
0
50
100
150
$\langle y \rangle^{\bar{\nu}}$
$E_{\bar{\nu}}$ (GeV)

FIG. 1

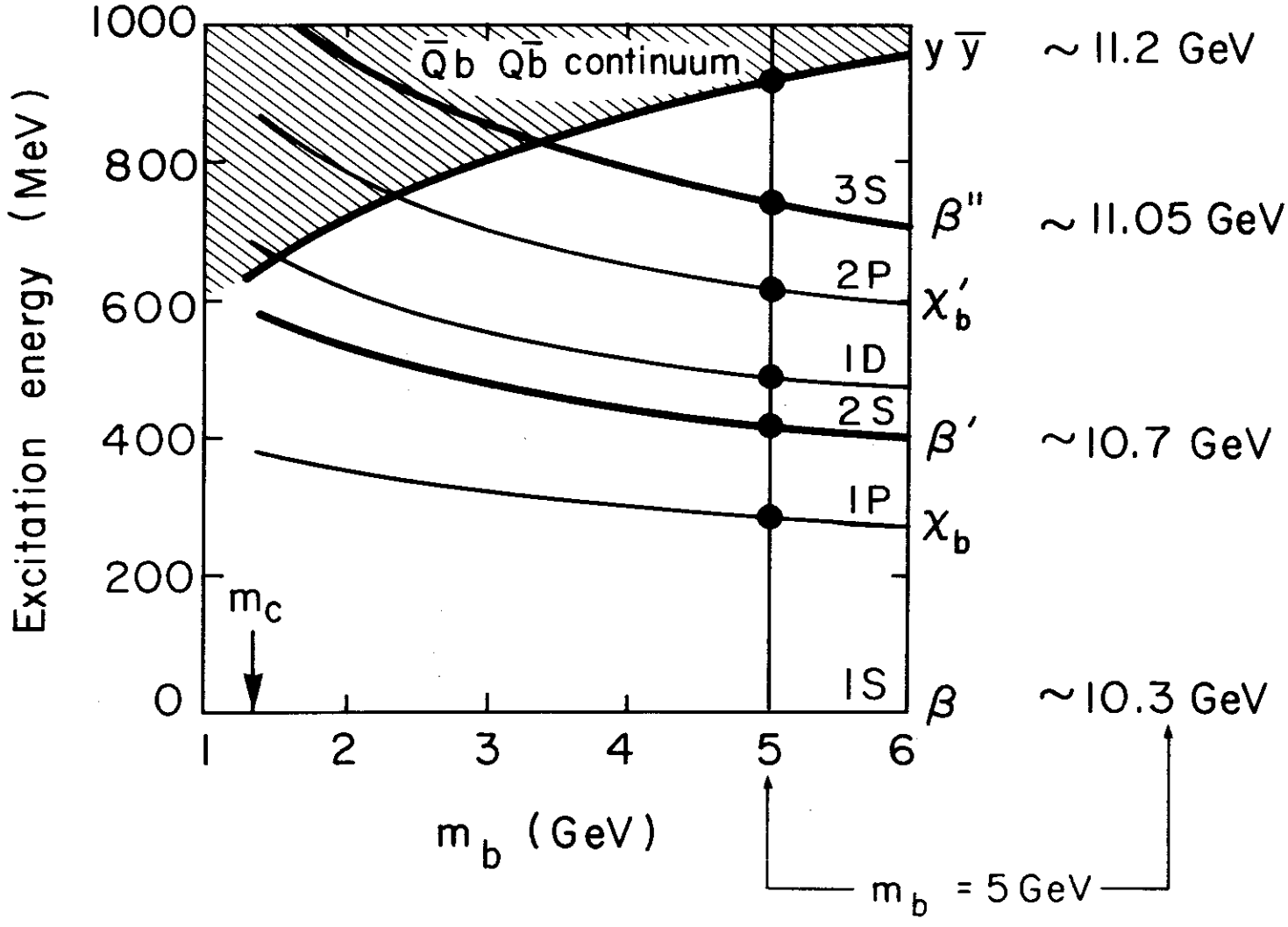
Excitation energy (MeV)
1000
800
600
400
200
0
$\bar{Q}b$ $Q\bar{b}$ continuum
$y\,\bar{y}$
~ 11.2 GeV
3S
β''
~ 11.05 GeV
2P
χ_b'
1D
2S
β'
~ 10.7 GeV
1P
χ_b
m_c
1S
β
~ 10.3 GeV
1
2
3
4
5
6
m_b (GeV)
m_b = 5 GeV

FIG. 2

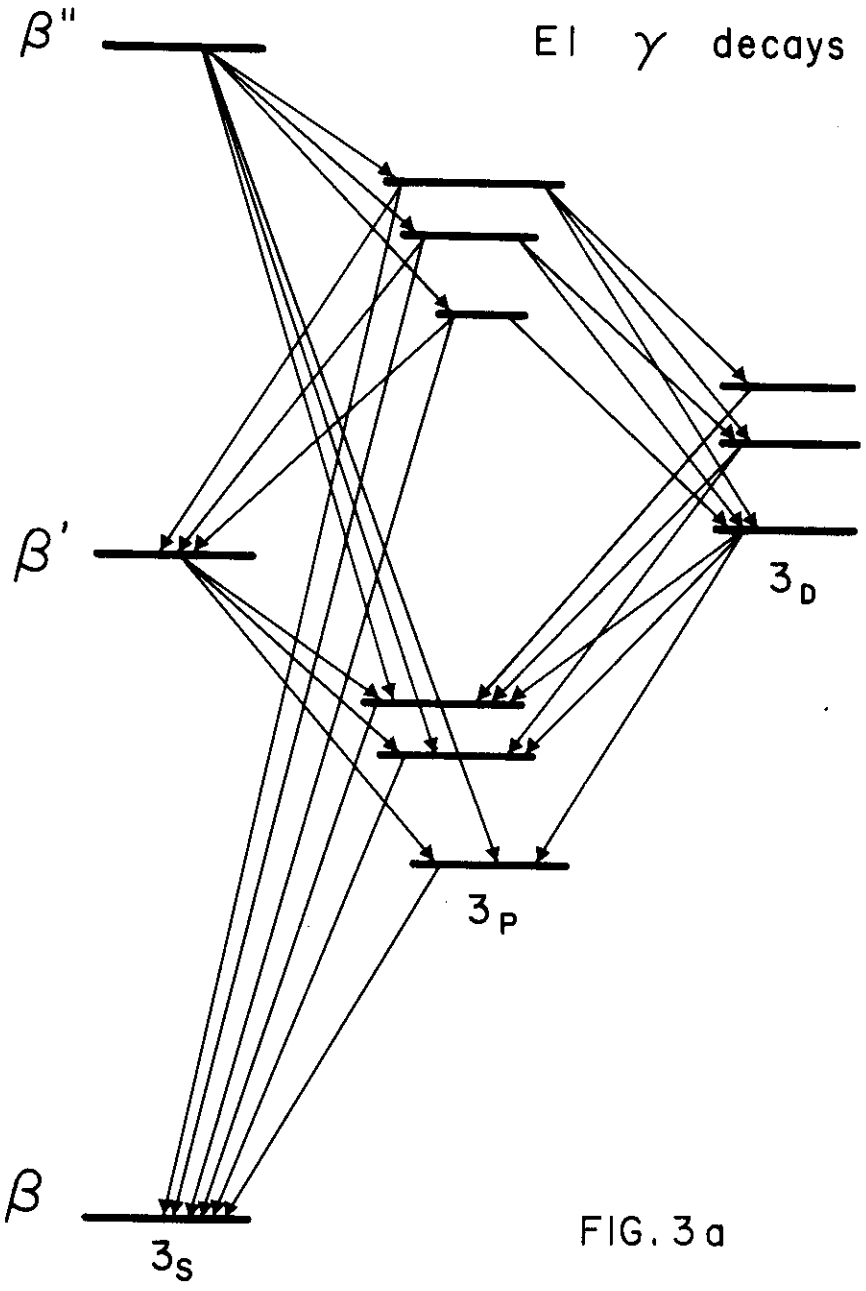

FIG. 3a

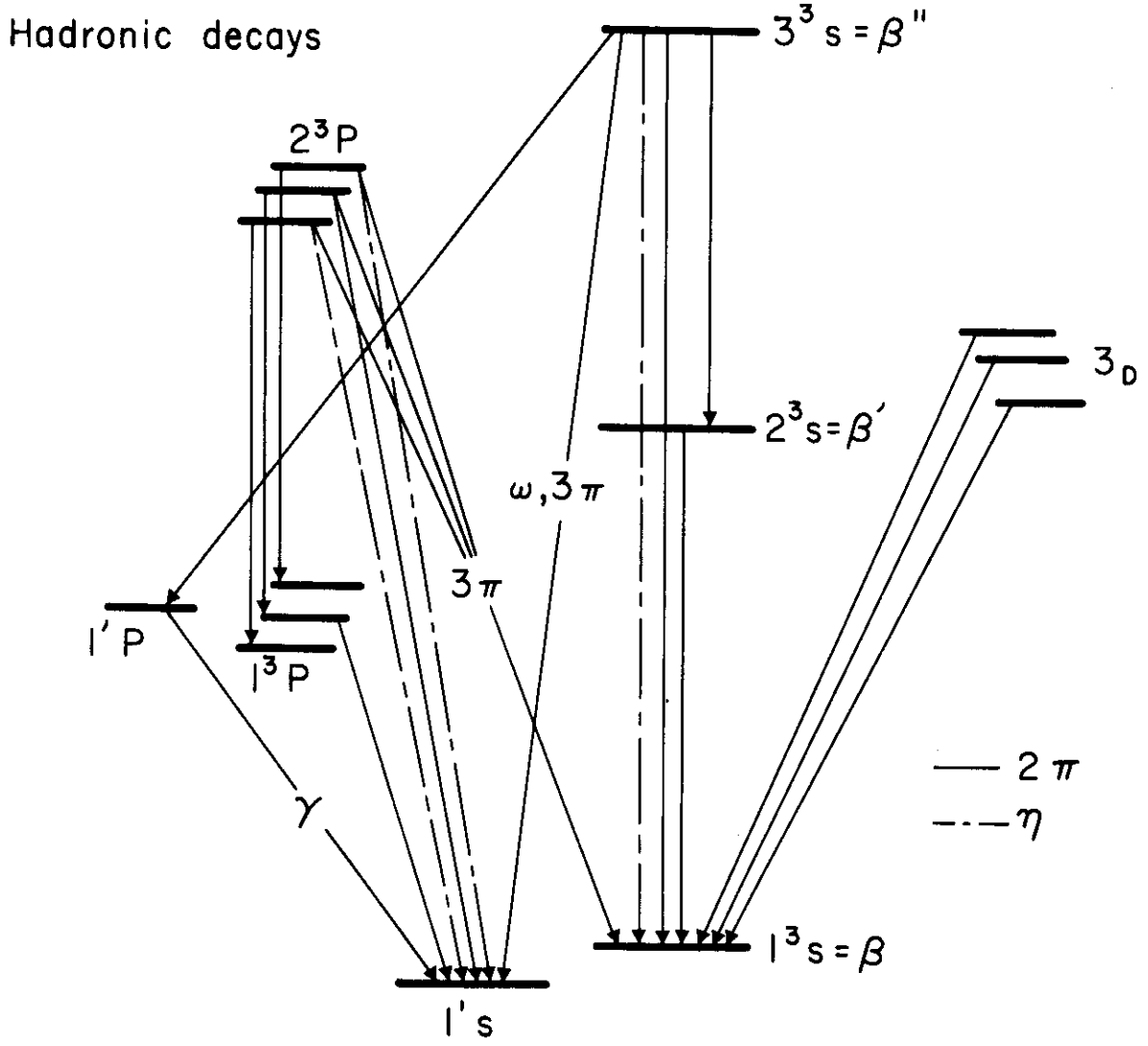
Hadronic decays
$3^3s=\beta''$
2^3P
3_D
$2^3s=\beta'$
$\omega,3\pi$
3π
$1'P$
1^3P
γ
2π
η
$1^3s=\beta$
$1's$

FIG. 3b

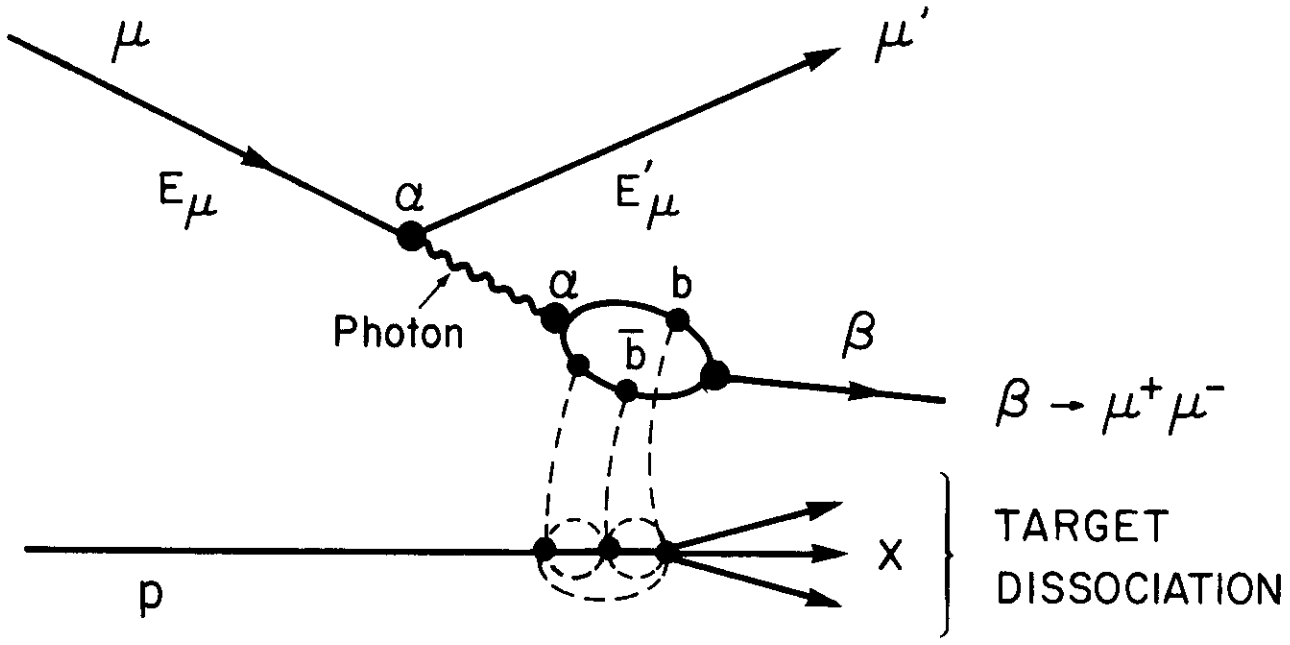

BASIC DIAGRAM OF β - PRODUCTION BY MUONS

FIG. 4

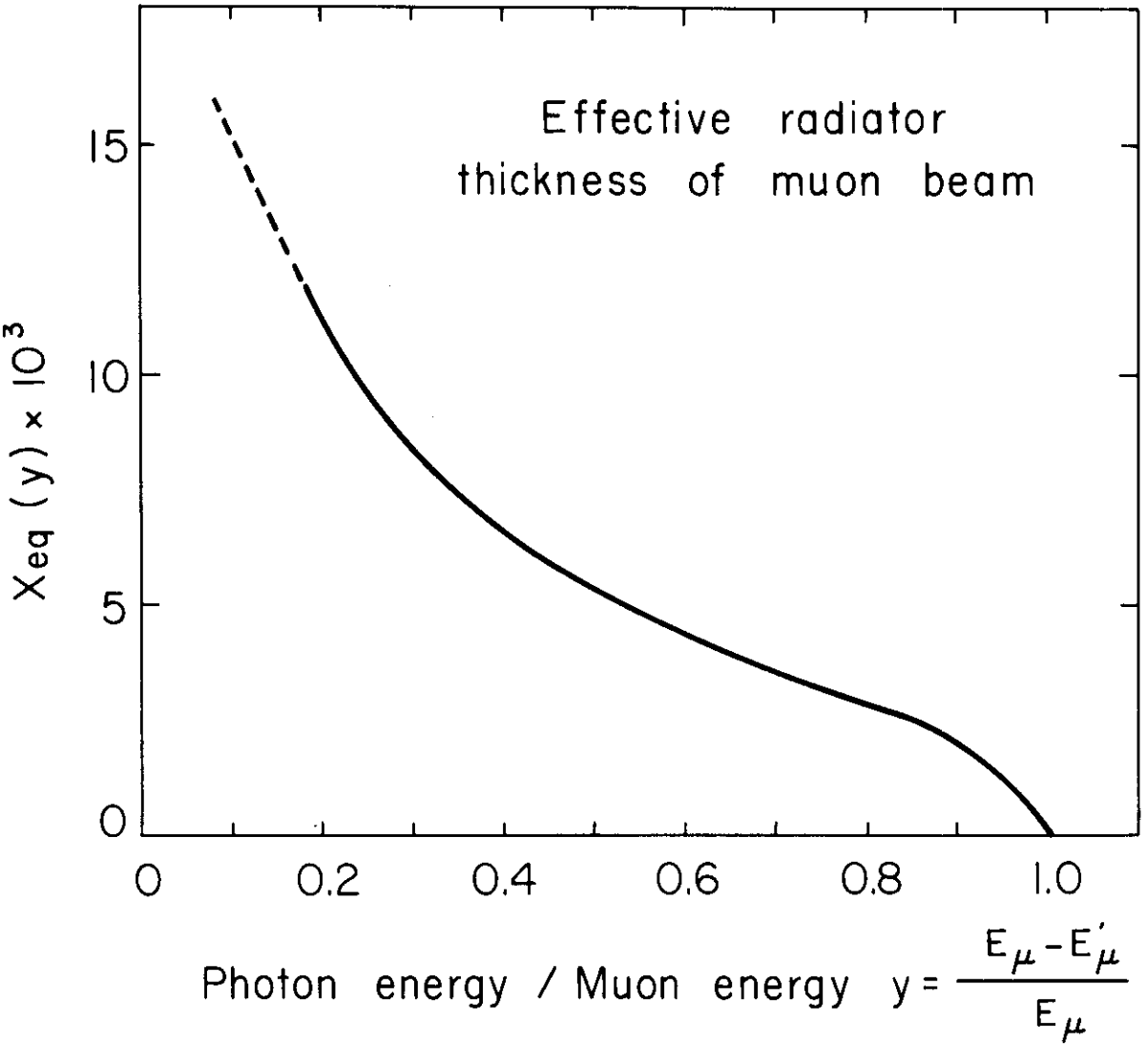
Effective radiator
thickness of muon beam
$X_{eq}(y) \times 10^3$
15
10
5
0
0
0.2
0.4
0.6
0.8
1.0
Photon energy / Muon energy $y = \frac{E_\mu - E'_\mu}{E_\mu}$

FIG. 5

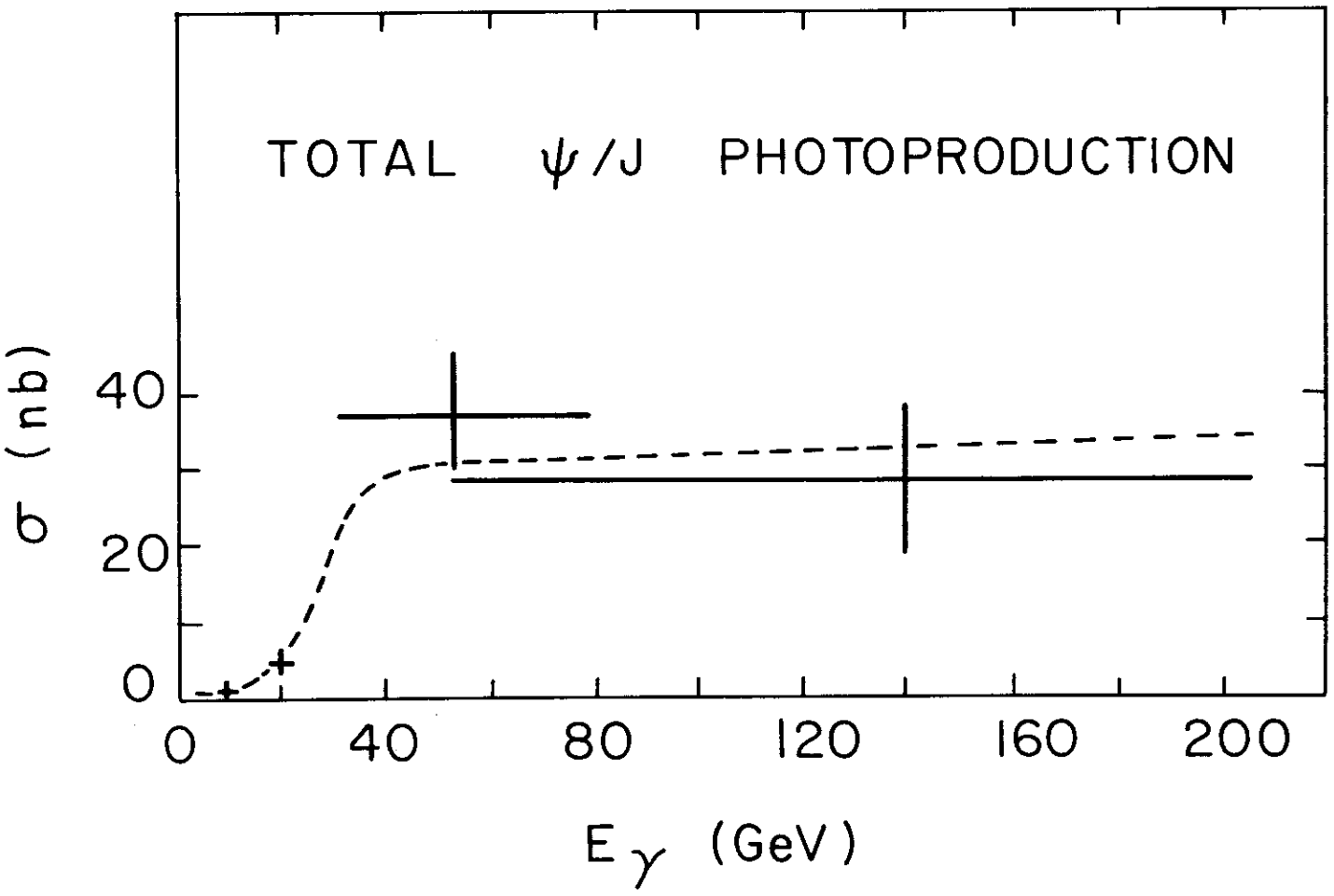

FIG. 6

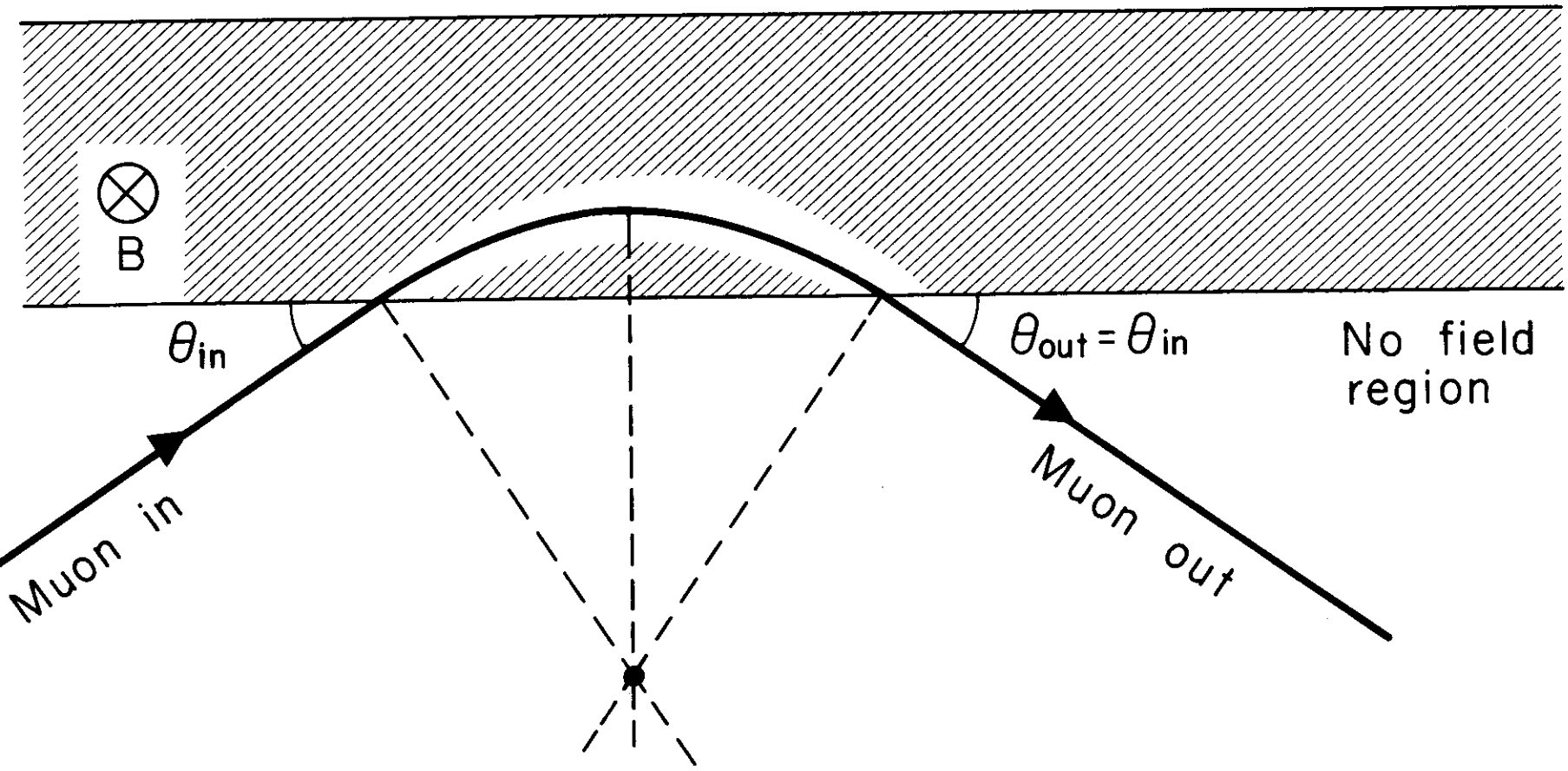

MIRROR ACTION OF A MAGNETIZED IRON PLATE

FIG. 7

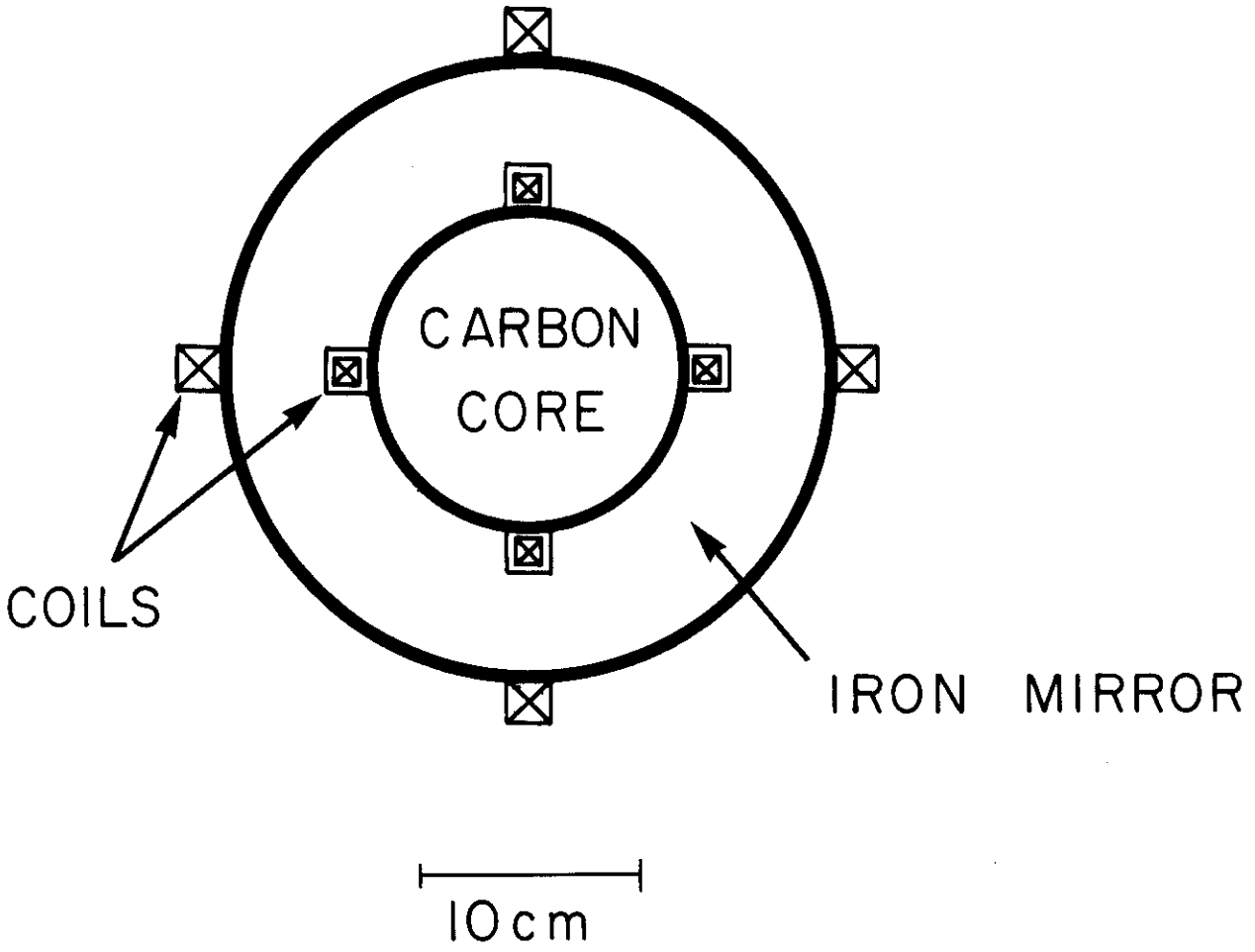

SCHEMATICS OF TARGET ARRANGEMENT

FIG. 8

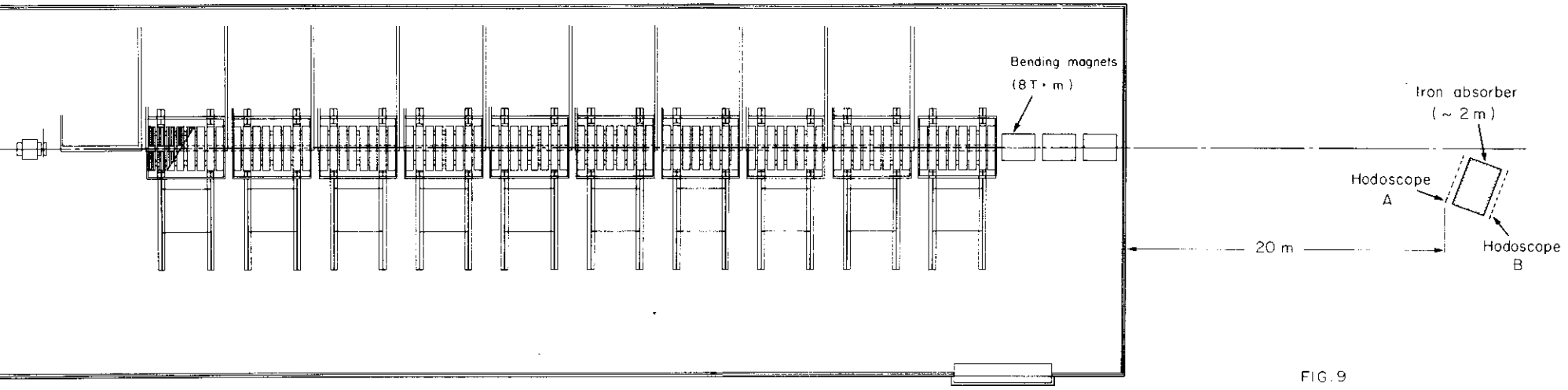

FIG. 9

NA 4 Experimental apparatus with added tagging telescope

TYPICAL EVENT

E_{inc} = 300 GeV $M_{\mu\mu}$ = 12 GeV E_{γ^*} = 150 GeV

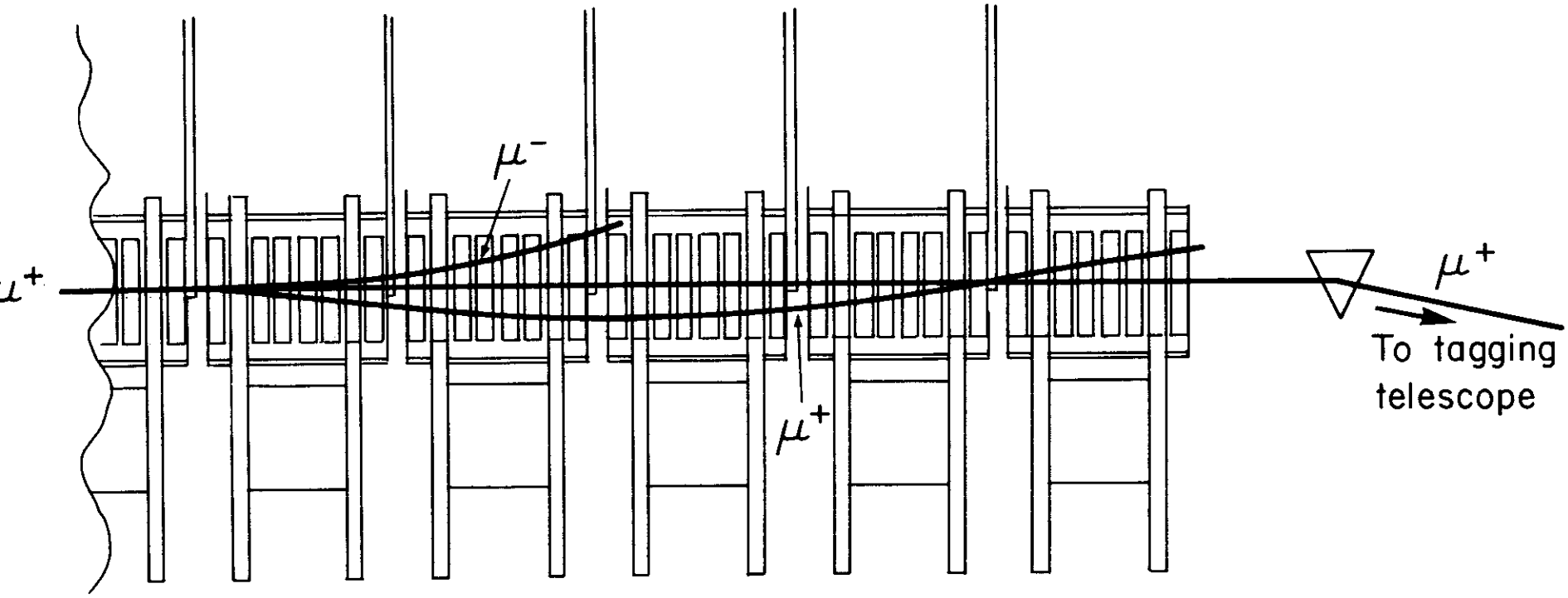

FIG. 10

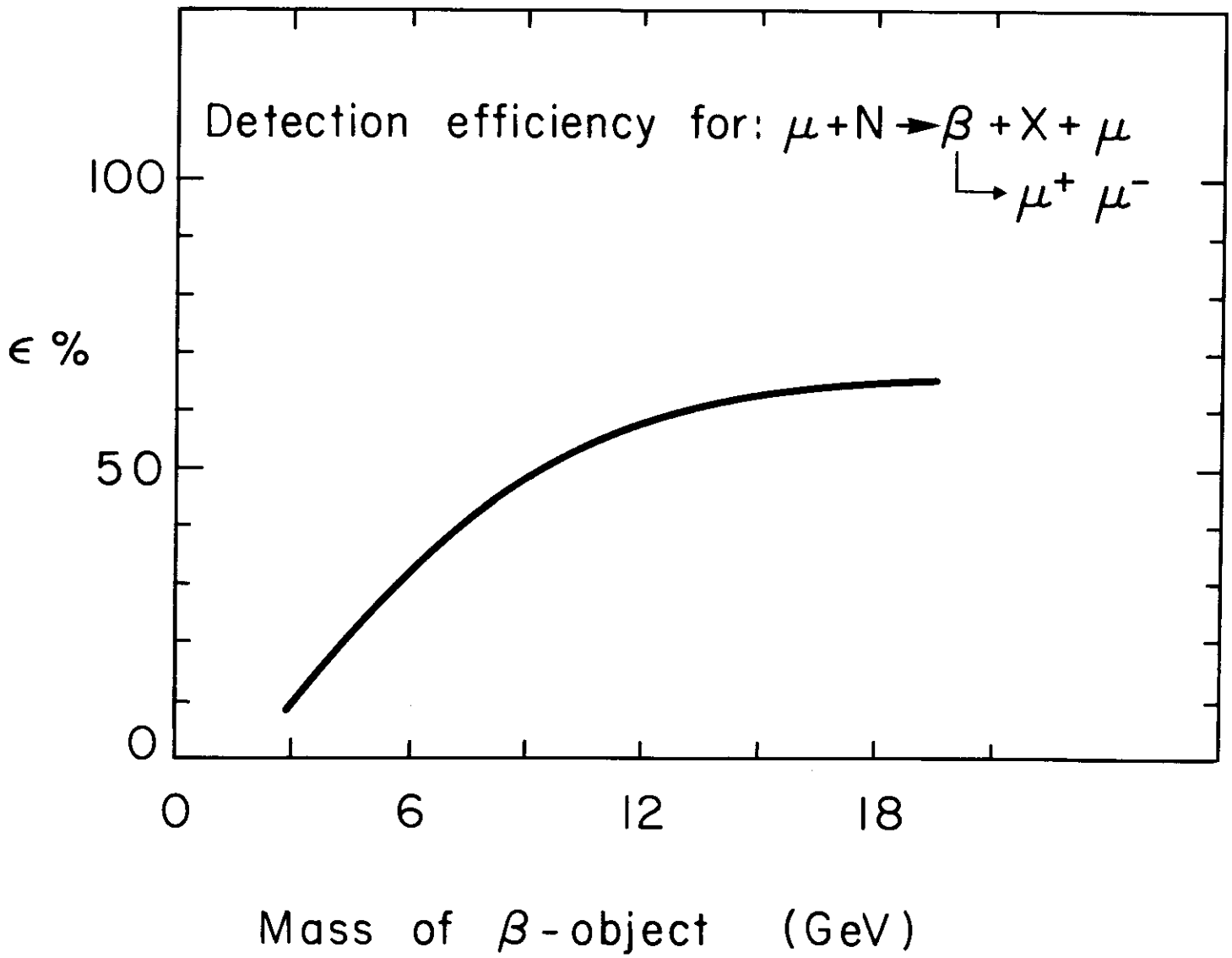
Detection efficiency for: $\mu + N \rightarrow \beta + X + \mu$
$\beta \rightarrow \mu^+ \mu^-$
100
50
0
ϵ %
0
6
12
18
Mass of β-object (GeV)

FIG. 11

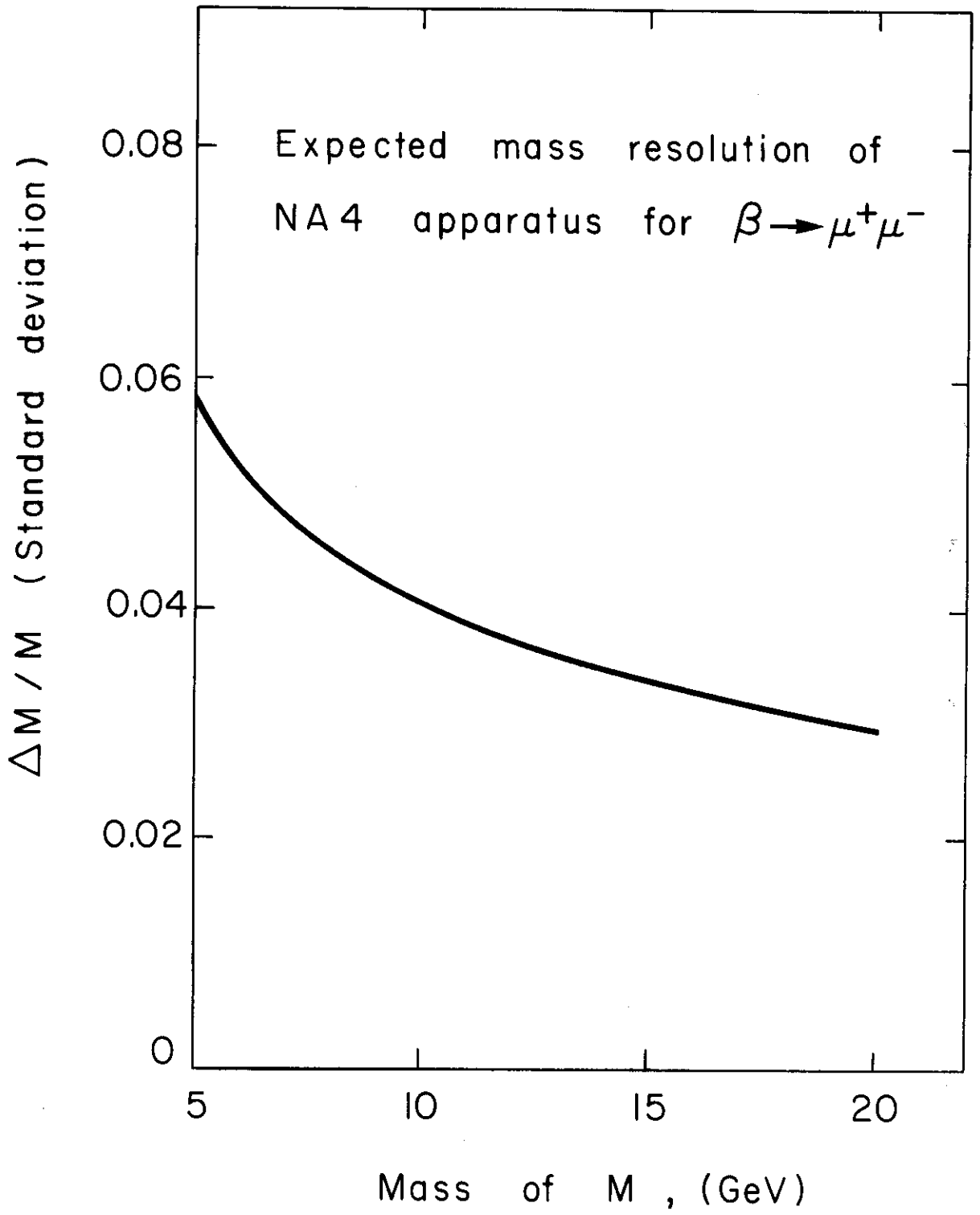
Expected mass resolution of
NA4 apparatus for $\beta \rightarrow \mu^+\mu^-$
0.08
0.06
0.04
0.02
0
5
10
15
20
ΔM / M (Standard deviation)
Mass of M , (GeV)

FIG. 12

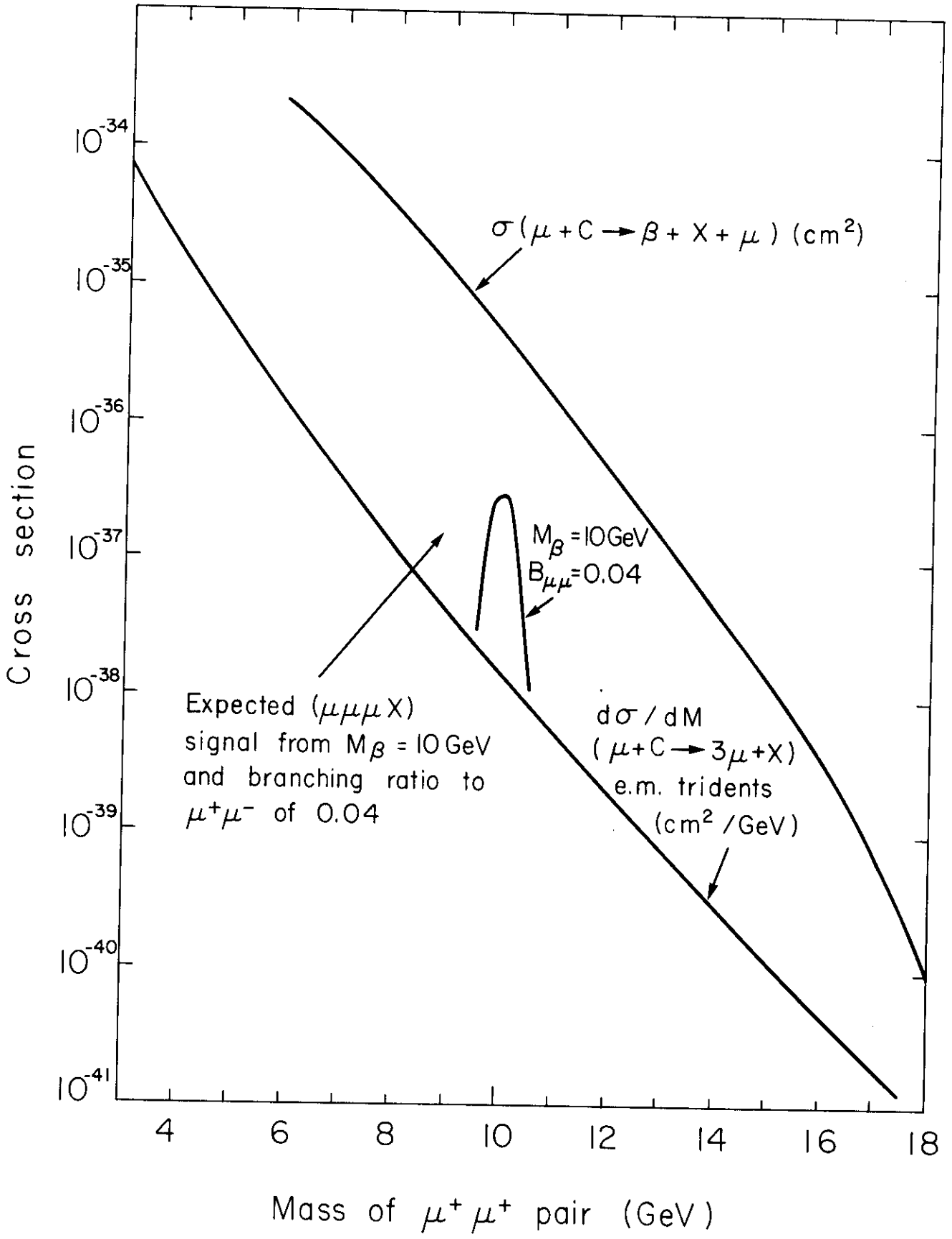
Cross section
10^{-34}
10^{-35}
10^{-36}
10^{-37}
10^{-38}
10^{-39}
10^{-40}
10^{-41}
$\sigma(\mu + C \rightarrow \beta + X + \mu)$ (cm^2)
M_β = 10GeV
$B_{\mu\mu}$=0.04
Expected ($\mu\mu\mu X$) signal from M_β = 10 GeV and branching ratio to $\mu^+\mu^-$ of 0.04
$d\sigma / dM$ ($\mu + C \rightarrow 3\mu + X$) e.m. tridents (cm^2 /GeV)
4
6
8
10
12
14
16
18
Mass of $\mu^+\mu^+$ pair (GeV)

FIG. 13